Pergamon

Int. J. Heat Mass Transfer. Vol. 39, No. 4, pp. 677–690, 1996

0017-9310/96 $15.00 + 0.00

0017-9310(95)00175-1

Determination of temperature field around a rapidly moving crack-tip in an elastic–plastic solid

WEN LI and XIAOMIN DENG†
Department of Mechanical Engineering, University of South Carolina, Columbia, SC 29208, U.S.A.

and

ARES J. ROSAKIS
Graduate Aeronautical Laboratories, California Institute of Technology, Pasadena, CA 91125, U.S.A.

(*Received* 1 *August* 1994 *and in final form* 16 *May* 1995)

Abstract—The problem of local heating and temperature rise induced by dynamic crack growth in elastic–plastic solids is studied numerically. Heat generation caused by plastic work dissipation is estimated from crack-tip stress and deformation fields obtained separately by two of the authors. The temperature field in an Eulerian description is shown to be governed by a convection-dominated flow equation with a singular source term that is distributed over an irregular crack-tip region, the active plastic zone. The peak value and spatial distribution of the temperature increase are determined using two independent computer codes, which are developed by the authors based on an integral representation of the temperature field and on an upwind finite element formulation. The accuracy and reliability of the numerical methods and their solutions are studied carefully against exact, closed-form solutions for several specially designed boundary value problems. These methods are used to simulate dynamic fracture tests on AISI 4340 steel specimens, and the predicted temperature contours and maximum values are found to be in good agreement with those measured and estimated experimentally.

1. INTRODUCTION

We communicate in this paper the results of our recent numerical study of temperature field induced by dynamic crack propagation in elastic–plastic materials. The success of this careful study, as detailed in the sequel, paves the road for more realistic, coupled and three-dimensional(3D) thermomechanical simulations of dynamic fracture events in structural metals. The broad objective of this study is to improve our understanding of the phenomena of local heating in structural metals induced by energy dissipation associated with dynamic crack propagation in metals. Since material properties usually depend on temperature and on the heating and cooling history experienced by the material, the magnitude, distribution and duration of crack-tip temperature rise as a result of crack-tip local heating can play a significant role in determining whether the crack will arrest or continue propagating and whether the crack will re-initiate growth after it has been arrested previously. From the point of view of structural design and evaluation against catastropic failures by dynamic fracture, a body of knowledge about what happens during dynamic crack propagation will have significant practical implications. To this end, it is noted that irreversible plastic work must be done in order to deform a solid inelastically. The energy consumed in doing such plastic work is accumulated in the active plastic zone and it usually dissipates into the surroundings in the form of heat. Experiments by Farren and Taylor [1] on aluminium, and by Taylor and Quinney [2] on copper show that about 90% of the plastic work turns into heat, and the rest is retained by the solid as stored energy (see [3]). When the rate of plastic deformation is sufficiently high, the heat generated cannot promptly diffuse away, thus causing rapid local heating and temperature increase. Since crack propagation is inherently a high strain rate event, fast crack growth in elastic–plastic solids is usually accompanied by severe crack-tip local heating and high temperature increase. In order to understand such thermomechanical phenomena in dynamic fracture, many investigators have strived to determine the peak value and spatial distribution of the temperature field during dynamic crack growth in elastic–plastic solids, such as metals.

In the area of experimental studies, Döll [4] was one of the earlier investigators who estimated the overall heat output at a propagating crack tip. From thermocouple measurements on four different polymer specimens, he found that the heat output due to plastic work increases with the crack speed. Fuller *et al.* [5] performed similar tests with liquid crystal films

† Author to whom correspondence should be addressed.

NOMENCLATURE

A	constant
B	constant
c	constant
D	nondimensionalized distributed heat source
E	Young's modulus
h	nondimensionalized finite element grid size
k	thermal conductivity [W m^{-1} K^{-1}]
K	dynamic stress intensity factor for crack propagation [MPa m$^{1/2}$]
m	Mach number, v/c_s
p	component of the Petrov–Galerkin finite element weighting function w
Pe	grid Peclet number, $ch/2$
q	nondimensionalized heat source distribution
Q	heat source distribution [W m^{-3}]
T	temperature rise [K]
v	crack propagation speed [m s^{-1}]
w	Petrov–Galerkin finite element weighting function
z	argument of K_0.

Greek symbols

α	thermal diffusivity [m^2 s^{-1}]
Γ	boundary of Ω
η	material parameter, the coefficient of plastic work convertion to heat
ρ	mass density [kg m^{-3}]
Ω	geometric domain
ξ, η	nondimensionalized x_1, x_2 coordinates of a point in the crack-tip active zone.

Mathematical symbols, superscripts and subscripts

$(\ )_{,\beta}$	$\partial(\ )/\partial x_\beta$, $\beta = 1, 2$
$\dot{(\ )}$	$\mathrm{d}(\ )/\mathrm{d}t$
c_p	specific heat [J K^{-1} kg^{-1}]
c_s	elastic shear wave speed [m s^{-1}]
f_T	constant
f_q	constant [K]
k_a	artificial diffusivity
K_0	the modified Bessel function of the second kind of order zero
n_β	unit outward normal vector of Γ
w_0	conventional Galerkin finite element weighting function
x_i	crack-tip coordinate system, $i = 1, 2$ [m]
x_i	nondimensionalized crack-tip coordinate system, $i = 1, 2$
σ_0	initial yield stress [Pa]
ε_0	initial yield strain
$\sigma_{\alpha\beta}$	stress tensor [Pa]
$\sigma_{\alpha\beta}$	nondimensionalized stress tensor
$\varepsilon^p_{\alpha\beta}$	plastic strain tensor.

and infrared detectors, as well as thermocouples. They estimated that the peak temperature rise near a crack that was growing at a speed in the range of 200–650 m s^{-1} was about 500 K. A more startling finding was reported by Weichert and Schönert [6] from radiation thermometer measurements, with a maximum temperature increase of 3200 K for cracks propagating in glass and 4700 K for cracks growing in quartz. More recently, Bryant *et al.* [7] conducted tests on two titanium alloys. They examined the fracture surface of test specimens using scanning electron microscopy and noticed droplet-like features at the rim of dimples of the fracture surface. They postulated that the droplets were the molten remnants of the micro-ligaments melted during the separation of the material. They concluded that the melting point of the titanium alloys can be exceeded during rapid crack propagation, where nearly adiabatic conditions exist.

An advanced experimental technique was recently developed and utilized successfully by Zehnder and Rosakis [8], which can be used to provide full-field type measurements of transient temperature distributions during dynamic crack propagation events. By focusing an array of eight high-speed, indium antimonide infrared (i.r.) detectors at points aligned vertically to the crack path of AISI 4340 carbon steel specimens, they were able to record the real-time temperature variations at all eight points (four on each side of the crack path) as the crack propagates with a speed of 1–2 km s^{-1}. The detectors they used can focus, without contact with the specimen, on a point with a small area of 0.16×0.16 mm^2. The points were spaced 0.2 mm apart along a line of approximately 1.56 mm in length. Hence the measurements obtained represent detailed and realistic temperature distributions around the running crack tip. Zehnder and Rosakis noted that the temperature near the crack tip can reach its peak value of about 500 K in just two microseconds (μs).

In the area of theoretical studies, models for estimating temperature rise and distribution in dynamic fracture have been proposed by a number of investigators (see [5, 9–15]). In the analysis by Rice and Levy [9], the classic Dugdale line-yield-zone model was employed to derive the crack-tip plastic work rate, which was used to estimate the peak temperature value, and in the study by Zehnder [10], the plastic work rate was estimated from consideration of dislocation motions. On the other hand, the plastic work rate was given an assumed form in [5, 11, 12] in the absence of mechanics solutions, and the temperature field was then calculated based on the assumed heat

input. In this connection, it is noted that the current trend in this area is to estimate the plastic work rate distribution directly from continuum mechanics analyses of the crack-tip stress and deformation fields. Li *et al.* [13] analyzed the case of *quasi-static*, anti-plane shear (mode III) crack growth in an elastic–plastic solid, with the plastic work rate and its zone of distribution derived from an analytic solution in the literature. The counterpart analysis of temperature rise for the case of *dynamic* mode III crack growth was performed by Douglas and Mair [14]. Sung and Achenbach [15] obtained a solution for the case of plane strain dynamic crack growth in an elastic-like viscoplastic solid, which was done with an adiabatic approximation and with the plastic work rate estimated from a crack-tip asymptotic analysis of the stresses and plastic strain rates. Since these studies do not directly model any actual crack growth tests, comparisons of their results with experimental measurements are not available. Qualitative analysis of the moving crack-tip temperature field variation, its gradient singularity, and the possible formation of shock waves have been performed extensively by Tzou (e.g. [16–18]).

In this and several earlier studies by the authors, a 2D finite element procedure has been developed to investigate both the mechanics problem and the associated energy dissipation and heat transfer problem with continuum mechanics concepts. This procedure is used to model actual dynamic crack propagation tests on 4340 steel specimens conducted at the California Institute of Technology. The accuracy and reliability of the procedure has been carefully examined at different stages of its development, both with existing analytical and numerical solutions and with experimental measurements. Results for the mechanics part of this study have been published previously (please refer to [19–24] for details) and will be described only briefly in this paper when necessary. Hence the emphasis of this paper is on the heat-transfer part of the modelling.

As delineated in subsequent sections, the temperature field induced by a moving heat source is governed by the same equation as that for a convection-dominated heat transfer problem. If a standard finite difference or finite element method is used to solve such a problem, erroneous node-to-node oscillations or divergence will arise unless unrealistically fine meshes are employed. Another numerical difficulty with the current heat-transfer problem is that the source term is distributed over an irregular region (the active plastic zone), is highly peaked (mathematically singular at the crack tip), and is travelling with the crack tip at a very high speed (of the order of 1 km s^{-1}). To overcome these numerical difficulties, a special finite element procedure is developed based on the Streamline Upwind Petrov–Galerkin Formulation (SUPG) [25, 26]. Since the accuracy of this formulation is only demonstrated in the literature for zero or uniformly distributed source terms, the procedure is carefully calibrated with specially designed boundary value problems that have distributed and peaked source terms and closed form solutions. To assure the accuracy of the procedure for problems without closed form solutions, an alternative numerical solution method based on an integral representation of the temperature field for a distributed moving heat source in an infinite domain is developed and used to generate results for comparison.

In this paper, we demonstrate that, when combined with a successive correction scheme for the solution of linear algebraic equations, the SUPG formulation can be extended with high accuracy and reliability to deal with convection-dominated flow problems, such as the present one, that have irregular source terms. We also demonstrate that the numerical integration method can be carried out accurately with an adaptive Simpson's integration algrithm as long as a certain parameter is below a critical value. The second approach, however, is much more expensive and less reliable. Finally, we will model actual dynamic fracture tests on AISI 4340 steel specimens. By taking into consideration the fact that about 90% of the total plastic work turns into heat, we obtained peak temperature values near the crack tip that match well with experimental measurements for crack speed ranging from 730 to 1140 m s^{-1}. The shapes of the computed temperature contours also resemble those estimated experimentally. Details are given below.

2. PROBLEM DESCRIPTION

We are concerned here with the problem of dynamic crack propagation in elastic–plastic solids that obey the von Mises yield criterion and the associated flow rule. To make the problem mathematically and numerically tractable, and to simulate the aforementioned dynamic fracture tests in two dimensions, our investigation is confined to the case of steady plane stress crack growth under small-scale yielding conditions, and all material properties involved will be treated as temperature independent, which enables less complicated, uncoupled mechanics and heat transfer analyses. Under the steady-state and small-scale yielding simplifications the problem becomes equivalent to that of a semi-infinite crack moving with a constant velocity in an otherwise infinite plate, and the crack-tip stress, deformation, and temperature fields are invarient to an observer who is sitting at the crack tip. The problem is illustrated in Fig. 1, with a moving and a fixed rectangular Cartesian coordinate system, where $a(t)$ is the crack length which depends linearly on time t and v is the crack propagation speed. For the purpose of numerical modelling, it has been found that a finite domain of sufficient size is enough for obtaining adequate solutions. Accordingly, we select a moving rectangular domain for the finite element mesh, as depicted in Fig. 2, where the size of the rectangle and the coordinates are made dimensionless by a normalization involving the applied stress inten-

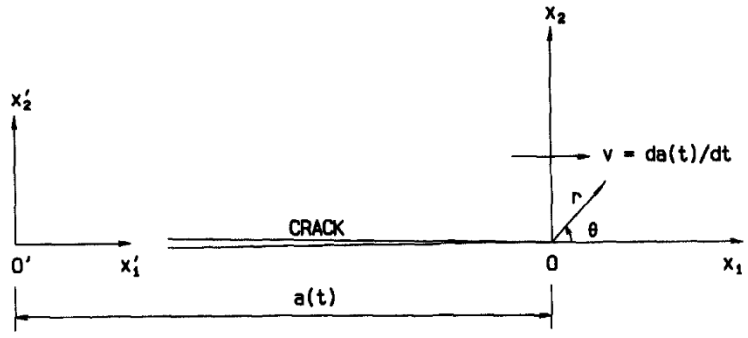

Fig. 1. A diagram of crack propagation, where (x_1', x_2') is a fixed reference coordinate system; (x_1, x_2) is a moving system with origin at the crack tip; and (r, θ) is the associated polar coordinate system.

sity factor K and the material's initial tensile yield stress σ_0. The nondimensional size of 4.5 for the domain, which is about 20 times that of the crack-tip active plastic zone, has been checked by the authors to be more than adequate for the present analysis. For example, the temperature field obtained by assuming this finite boundary is found to be almost identical to that obtained by assuming an infinite boundary (see, for example, Fig. 6, where the small difference in front of the crack tip is explained in Sections 3.3 and 4.1).

2.1. *Heat transfer equation*

With respect to the moving coordinate system, the governing equation for the temperature field T of the heat transfer problem induced by dynamic crack growth in elastic–plastic solids is

$$kT_{,\beta\beta} + Q = \rho c_p \dot{T} \tag{1}$$

where k is the thermal conductivity, ρ the mass density, c_p the specific heat, Q the internal heat generated per unit time per unit volume. Indicial notations and its associated conventions are adopted both here and in the sequel, with Greek indices having values 1 and 2. Hence, subscripts following a comma denote spatial partial differentiation and repeated indices imply summation. Also, a dot over a variable means material time differentiation, which for the case of steady crack growth can be related to the spatial partial derivative $(\ )_{,1}$ to $(') = -v(\ )_{,1}$. Consequently, the heat transfer governing equation can be put in the following form

$$T_{,\beta\beta} + (v/\alpha)T_{,1} = -Q/k \tag{2}$$

where $\alpha = k/\rho c_p$ is the thermal diffusivity.

2.2. *Heat source distribution*

Since heat is generated by means of the consumption of plastic work, the heat source term Q is distributed only over the crack-tip active plastic zone, which translates with the propagating crack tip but is stationary if viewed in the moving coordinate system. The shape of the crack-tip plastic zone under small-scale yielding conditions and for several classes of elastic–plastic materials is available for various crack propagation speeds from [21–23]. The case shown in Fig. 3 is from [21] for a linear hardening solid, where the hardening coefficient α, which is different from that used for thermal diffusivity, is the ratio between the slope of the plastic stress–strain line and that of the elastic stress–strain line (the Young's modulus), and $m = v/c_s$, the Mach number, is the ratio of the crack speed over the material's elastic shear wave speed. At each point of the active plastic zone, Q equals a fraction of the total plastic work rate and can

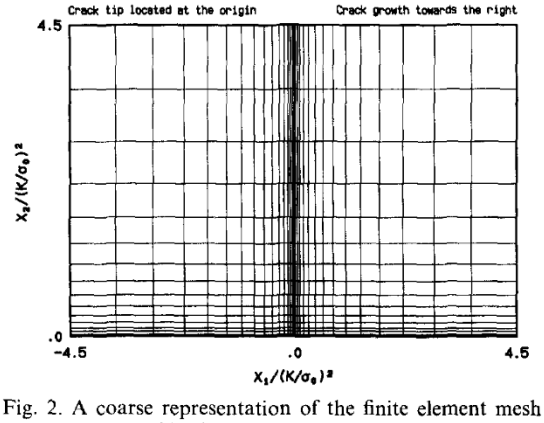

Fig. 2. A coarse representation of the finite element mesh used in the present computation.

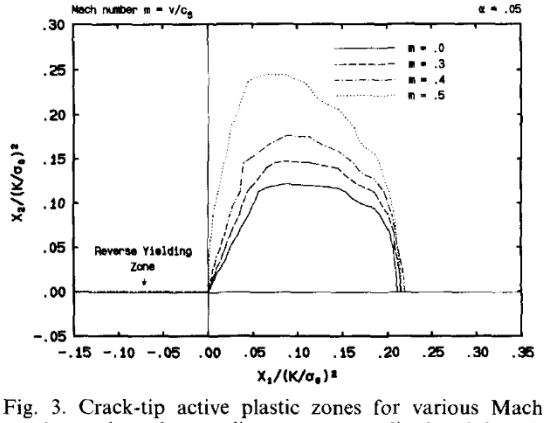

Fig. 3. Crack-tip active plastic zones for various Mach numbers, where the coordinates are normalized and the origin is at the crack tip (from ref. [22]).

be derived in terms of the stress and plastic strain rate fields as

$$Q = \eta \sigma_{\beta\gamma} \dot{\varepsilon}^{\mathrm{p}}_{\beta\gamma} = -\eta v \sigma_{\beta\gamma} \varepsilon^{\mathrm{p}}_{\beta\gamma,1} \tag{3}$$

where $\sigma_{\beta\gamma}$ and $\varepsilon^{\mathrm{p}}_{\beta\gamma}$ denote respectively the 2D stress and plastic strain tensor components, and the coefficient η is a material parameter that measures the ratio of plastic work convertible to heat. For metals, η has been shown experimentally to be around 0.9.

Besides its peculiar region of distribution, the heat source associated with dynamic crack propagation in elastic–plastic solids has another special feature. As shown in [21–23], the stress and/or plastic strain fields are always mathematically singular at the crack tip, which represents the asymptotic tendency of the mechanics fields when the crack tip is approached. As such, the resulting heat distribution function Q is also singular at the crack tip, although the induced temperature field is bounded there. For ideally plastic solids, linear hardening solids and power-law hardening solids, Q can be calculated according to equation (3) from the stress and plastic strain fields from separate studies by two of the authors [21–23].

2.3. *Nondimensional normalizations*

For the sake of generality, the stress and deformation fields in [21–23] have been obtained in nondimensional forms, which is made possible with the use of special normalizations. In order to utilize the same finite element mesh as that used for the stress analysis and to derive the plastic work rate from the mechanics fields, we adopt those special normalizations here. Hence we normalize the coordinates with $(K/\sigma_0)^2$, the crack speed with c_s, $\sigma_{\beta\gamma}$ with σ_0, and $\varepsilon^{\mathrm{p}}_{\beta\gamma}$ with ε_0 where ε_0 is the ratio between σ_0 and the Young's modulus E. It is understood that, unless specified otherwise, subsequent appearances of these variables are in the nondimensional forms. However the Mach number m will be used in place of the normalized crack speed v. With these normalizations, the governing equation (2) can be re-written in terms of the nondimensional coordinates, stresses, and plastic strains as follows

$$T_{,\beta\beta} - f_{\mathrm{T}} T_{,1} = f_{\mathrm{q}} q \tag{4}$$

where

$$f_{\mathrm{T}} = -\frac{K^2 m c_s}{\alpha \sigma_0^2} \quad f_{\mathrm{q}} = \frac{K^2 m c_s}{kE} \quad q = \eta \sigma_{\beta\gamma} \varepsilon^{\mathrm{p}}_{\beta\gamma,1}. \tag{5}$$

Equation (4) is in fact the governing equation for convection–diffusion type flows, where the first term on the left represents diffusion (heat conduction) and the second term, convection. The numerical solution corresponding to properly posed boundary conditions will be the subject of the following sections. It must be noted that, to an observer who is moving with the crack-tip coordinate system, the material particles are flowing downstream in the opposite direction of crack growth (the flow is along the negative x_1-axis in Fig. 1). It is noted that the coefficient f_{T} is a nondimensional constant and f_{q} is a constant with the dimension of the temperature, and both are directly proportional to the Mach number m. The magnitude of f_{T} is a measure of the amount of heat convection induced by the moving heat source at the crack tip vs that of heat conduction in the bulk material during dynamic crack growth.

In structural metals, such as AISI 4340 carbon steel, the absolute value of f_{T} is usually very large when the crack speed is a fraction of the elastic shear wave speed. For example, the 4340 steel has the following relevant parameter values: $E = 200$ GPa, $\sigma_0 = 1.49$ GPa, $c_s = 3200$ m s^{-1}, $k = 38.1$ W (m K)$^{-1}$, $\alpha = 1 \times 10^{-5}$ m^2 s^{-1}. The critical stress intensity factor value (the dynamic fracture toughness) of the material at $m = 0.22$ is approximately $K = 90$ MPa$\sqrt{m}$ according to the experimental measurements by Zehnder and Rosakis [28]. When the above parameter values are used, f_{T} is found to be on the order of 10^5 (as a comparison, f_{q} is on the order of 10^6 for this case). In this connection, an interesting observation can be made from equations (4) and (5) as to how T depends on K, m and other material parameters. It is noted that, when m and hence f_{T} are sufficiently large, the left-hand side of equation (4) is dominated by the convection term. Hence it appears that T is almost proportional to the ratio between f_{T} and f_{q}. Since f_{T} and f_{q} are identically proportional to K and m, the dependence of T on K and m via the ratio $f_{\mathrm{T}}/f_{\mathrm{q}} = -\alpha\sigma_0^2/kE$ disappears. Thus this dependence, if any, must come from the product represented by q. However, it is noted that the function q in the nondimensional coordinate system depends only on m and not on K and other material parameters listed above. As such, it is concluded that T in the nondimensional coordinate system is almost independent of K, and its dependence on m derives from those of the stress and plastic strain fields and from that of the crack-tip active plastic zone. Other material parameters are expected to influence T mainly through the lumped factor $\alpha\sigma_0^2/kE$.

2.4. *Boundary conditions*

As stated earlier, we will model the dynamic fracture tests conducted on AISI 4340 steel plate specimens, including crack-tip local heating and temperature distribution. We note that, when the heat source is moving rapidly with the crack tip, the near-tip temperature variation is mainly determined by heat convection due to the moving heat source, and partially influenced by heat conduction through the bulk material. It is therefore reasonable to conclude, on the time scale of this problem, that the effect of heat loss due to heat convection and radiation on the two bounding surfaces of the plate can be neglected. Hence we only need to consider conditions that may be imposed on any boundaries in the x_1–x_2 plane. Apparently, in the case of an infinite domain, the boundary conditions are given by zero temperature rise or $T = 0$ at

infinity. If a finite domain is used to simulate the infinite domain problem, then proper conditions must be specified such that the near-tip temperature distribution is unaffected by this finite domain approximation. In this study, for the moving rectangular domain mentioned earlier (see Fig. 2), temperature increase along the vertical boundary ahead of the crack is set to zero. This is because temperature rise ahead of a rapidly propagating crack is practically determined by local heating due to energy dissipation in the crack-tip plastic zone. In this study, the vertical boundary ahead of the crack is located sufficiently away from the crack-tip plastic zone so that a zero temperature rise is expected. Along the rest of the boundary the heat flux (normal temperature gradient) is set to zero. For the bottom boundary this is because it is a symmetry line. For the left boundary, this is because it is a downstream boundary and is sufficiently away from the dominant heat source at the crack tip. Similarly for the top boundary, this is because it is found to be sufficiently far away from the crack tip so that the temperature variation there is very slow. We have examined with satisfaction the accuracy of the boundary conditions chosen above by extensive comparisons with results calculated for the infinite domain case. An example is shown in Fig. 6, where temperature rise along the x_1 or x-axis is given. The SUPG finite element solution is for the finite domain, and the numerical integration result is for the infinite domain. It is clear that the temperature distributions are almost identical up to the left boundary. The difference ahead of the crack tip is physically insignificant and is due to the difficulty of the numerical integration method right ahead of the crack tip (see discussions in Sections 3.3 and 4.1).

3. COMPUTATIONAL ASPECTS

It is clear from the earlier discussions that we need to solve a 2D boundary value problem for a field variable T that is governed by a partial differential equation of the form

$$T_{,\beta\beta} - cT_{,1} = D \tag{6}$$

where c is a constant and D is a distributed source term. Without loss of generality, we assume that the coordinates have been nondimensionlized so that c is dimensionless and D has the same dimension as T. This is the governing equation for a convection–diffusion flow in x_1-direction and the constant c can be referred to as the dimensionless flow speed. We point out that the direction of flow is along the positive x_1-axis if $c > 0$ and along the negative x_1-axis if $c < 0$. When $|c|$ is sufficiently large, equation (6) governs the so-called convection-dominated flow problems. For the dynamic crack growth induced heat transfer problem in metals, c is of the order of 10^5.

When $|c| \gg 1$, fictitious numerical oscillations in the flow direction will arise if standard finite difference or finite element methods are used to calculate the solution for such a boundary value problem. Although this problem can be corrected by reducing the element size of the mesh, it would require the mesh to be unrealistically fine. This numerical performance versus element size relationship is dictated by the mesh or grid Peclet number Pe [26, 27], given by

$$Pe = ch/2 \tag{7}$$

where h is the dimensionless element size in the flow direction. Spurious oscillations will arise when $Pe > 1$. For the dynamic crack growth problem, this node-to-node oscillation can be avoided only if the mesh size is on the order of 10^{-5} (since c is of the order of 10^5), which would make the numerical modelling task impractical. To overcome this numerical difficulty, an upwind technique known as the Streamline Upwind Petrov–Galerkin Formulation (SUPG) [25–27] is adopted here. This formulation has been shown to work well for convection-dominated flow problems in one and two dimensions with zero or constant source terms.

3.1. *Streamline upwind Petrov–Galerkin formulation*

The SUPG formulation [25–27] as it applies to equation (6) is specified here. In this formulation the weighted residue statement on a domain Ω is written as

$$\int_\Omega w(T_{,\beta\beta} - cT_{,1} - D)\,\mathrm{d}\Omega = 0 \tag{8}$$

where w is a weighting function, which can be expressed as the sum of a conventional Galerkin weighting function, say, w_0, and a perturbation term p, which is given in terms of w_0 by

$$p = k_a w_{0,1}/c. \tag{9}$$

The dimensionless constant k_a in equation (9) is called the artificial diffusivity and should be positive. Its value must be chosen properly in order to obtain the best performance. Following the arguments by Christie *et al.* [29] for 1D flows and by Hughes and Brooks [26] for multi-dimensional flows, the expression below can be derived to provide the optimal value for k_a:

$$k_a = \frac{ch}{2}\left(\coth(Pe) - \frac{1}{Pe}\right) = Pe\coth(Pe) - 1 \tag{10}$$

where Pe, the grid Peclet number, is determined from (7).

A weak form for equation (8), which will be the basis of our finite element discretization, can be written as

$$\int_\Omega [(1+k_a)w_{0,1}T_{,1} + w_{0,2}T_{,2} + w_0 cT_{,1}]\,\mathrm{d}\Omega = -\int_\Omega wD\,\mathrm{d}\Omega + \int_\Gamma wn_\beta T_{,\beta}\,\mathrm{d}\Gamma \tag{11}$$

where Γ stands for the part of the boundary of Ω where the normal gradient of T, given by the product $(n_\beta T_{,\beta})$, is specified, and n_β represents the components of the outward unit normal vector of Γ. It is important to note that the Galerkin weighting function w_0 is operating on the left-hand side of (11) while the SUPG weighting function w is operating on the right, which is the main difference between SUPG and the earlier upwinding techniques. When k_a is set to zero, the conventional Galerkin formulation is recovered.

A schematic of the finite element mesh used in this study is shown in Fig. 2, where four-noded quadrilateral elements are focused near the crack tip, so that large gradients of the near-tip stress, deformation, and temperature fields can be adequately represented. The mesh is designed based on the need of the stress analysis, but it is also shown to be adequate for the temperature analysis, as discussed later. The actual mesh is composed of a 60×30 grid. The size of the largest element is 0.7636 while that of the smallest element is 0.3748×10^{-4}. A standard finite element discretization procedure then leads to a set of linear algebraic equations. The resulting stiffness matrix is asymmetric because of the convection term, $cT_{,1}$, in equation (11). As a comparison, it is noted that the stiffness matrix from the conventional Galerkin formulation is always symmetric. In order to obtain solutions with desired accuracy, we find it necessary to solve the linear algebraic equations with a successive correction scheme.

3.2. *Comparison with conventional Galerkin formulation*

Comparisons between the SUPG formulation and the conventional Galerkin formulation for convection-domated flow problems are available in the literature for one dimensional cases and with zero and constant source terms [26, 30]. In order to demonstrate the applicability and effectiveness of the SUPG formulation to multi-dimensional problems with general source terms, we will analyze a test problem with both methods. The test problem is governed by equation (6) and is defined on the nondimensional rectangular domain shown in Fig. 2. The source term D is distributed over the entire domain according to the expression below

$$D(x_1, x_2) = -2cx_1 + 2x_2 - (2.5 + 9c) \qquad (12)$$

where the constant c is identical to that in equation (6) and is used here as a parameter. When the governing equation is accompanied by the boundary conditions

$$T_{,1} = 0 \text{ along } x_1 = -4.5, \quad T_{,2} = 0 \text{ along } x_2 = 0,$$

$$T_{,2} = 0 \text{ along } x_2 = 4.5,$$

$$T = 81 - 2.25x_2^2 + x_2^3/3 \text{ along } x_1 = 4.5 \qquad (13)$$

the solution for T over the rectangular domain can be represented exactly by

$$T(x_1, x_2) = (4.5 + x_1)^2 - 2.25x_2^2 + x_2^3/3. \qquad (14)$$

It must be pointed out that the above specially devised boundary value problem has a solution that is independent of the parameter c, so that one can realize a wide range of Peclet numbers with a fixed element size by simply setting c to different values. In addition, one can observe how the SUPG formulation and the conventional Galerkin formulation behave as the Peclet number increases. As is known from analyses in the literature, solutions from the conventional methods are usually useless when the Peclet number is larger than one. However, it happens that, for the test problem with a mesh to be described, the solution given by the conventional Galerkin formulation remains reasonable for Pe up to nearly 100, then it becomes divergent and overflows during computation when Pe goes higher. On the other hand, the solution obtained with the SUPG formulation consistently gives very accurate solutions.

A comparison is shown in Fig. 4 for the variation of T in the x_1 direction for the case of $c = 100$. The rectangular domain is uniformly divided into a 6×3 grid, giving rise to 18 square elements of size $h = 1.5$, and resulting in a Peclet number of $Pe = 75$, so this is a very coarse mesh. It is amazing at first glance that for such a coarse mesh and with such a large Peclet number, the conventional Galerkin formulation still yields overall a very reasonable solution, as demonstrated in Fig. 4(a) by the comparison at the nodal points with the exact solution, where the variation of T is shown along the x_1-axis. It is believed that this 'good behavior' is fostered by the favorable boundary condition of large prescribed values of T along the boundary $x_1 = 4.5$. However, at places where T is small, a node-to-node oscillation can be observed, as shown in Fig. 4(b) for the variation of T along $x_2 = 3.0$. A remarkable feature of this oscillation is that the error it produced over the entire rectangular domain forms a periodic cylinderical surface parallel to the x_2-axis, which resembles a stationary wave along the x_1-axis. Figure 4(c) shows a profile of this error surface in the x_1 direction. In contrast, the SUPG method always gives nodally exact solutions even for such a coarse mesh, except along the boundary $x_1 = -4.5$ where small errors exist, which is believed to be caused by the coarse mesh and the inflow gradient boundary condition there.

3.3. *Comparison with numerical integration approach*

As discussed earlier, the distributed source term associated with the temperature field induced by dynamic crack propagation in elastic–plastic solids is strongly peaked at the origin, where its gradient is exceedingly large. Such a source term presents a special numerical difficulty by itself, since the solution of the governing equation is very much dictated by the source term, hence very sensitive to error introduced in the numerical representation and integration of the distributed source term. Great care must be taken in handling such numerical procedures. In order to verify that the finite element mesh designed in [19], and

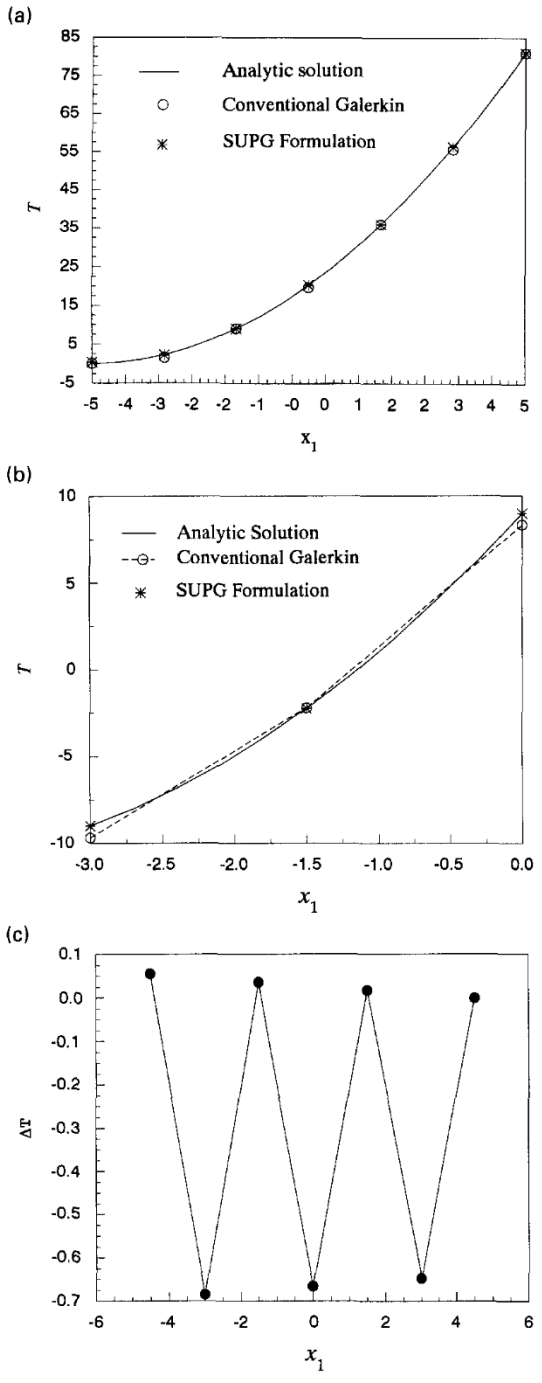

Fig. 4. Comparisons between analytic and numerical solutions: (a) variation of T along x_1-axis; (b) variation of T along $x_2 = 3.0$; (c) variation of error in T from the conventional Galerkin formulation.

shown schematically in Fig. 2, can be adopted to obtain the temperature field accurately and reliably with the SUPG formulation, a test problem that has a highly peaked source term and an exact, closed-form solution must be devised.

Another way to check the reliability of the SUPG program is to establish an alternative, independent approach to solve the temperature field and compare the solution with SUPG. Such an alternative method indeed exists and in fact has been used, for example, in a theoretical study of the temperature field for mode III crack growth in [14]. This method is valid for calculating the temperature field in an infinite plane induced by a constant heat source moving with a constant speed in a fixed direction. Based on the fundamental solution for a unit moving point heat source [31], the solution for equation (6) for an infinite domain is given by

$$T(x_1, x_2) = \int\int_{\Omega} \frac{D(x_1, x_2)}{2\pi} \exp\left(\frac{c(x_1 - \xi)}{2}\right) \times K_0\left(\frac{|c|}{2}\sqrt{[(x_1 - \xi)^2 + (x_2 - \eta)^2]}\right) d\xi\, d\eta \quad (15)$$

where exp( ) refers to the exponential function, and K_0( ) the modified Bessel function of the second kind of order zero [32].

However, a severe numerical complication will be encountered in evaluating equation (15) when the dimensionless parameter c is sufficiently large. This numerical difficulty arises because of a peculiar feature of the product $\exp(u)K_0(z)$, where u is used to denote the argument of exp, and z the argument of K_0, in the integrand of (15). For example, consider the case when the nondimensional distance d between (ξ, η), a heat source point, and (x_1, x_2), a point where T is to be calculated, is larger than or equal to 2. When $\xi < x_1$, $\exp(u)K_0(z)$ decays exponentially as d increases, and when $\xi > x_1$, $\exp(u)K_0(z)$ decays exponentially as the difference $|\eta - x_2|$ increases. In both cases, the decaying rate is given by $c/2$. For the problem of dynamic crack growth, c is on the order of 10^5, an incredibly large number. As such, for the 9×4.5 rectangular domain, the main contribution to T must come from the distributed source in a narrow band parallel to the x_1-axis, whose width is on the order of 10^{-5}. In addition, the integrand of (15) still has a very deep slope in all directions even within this tiny band! Imagine the amount of care and effort needed to calculate the temperature distribution according to the integral representation in (15). Besides, how does one assure oneself that the numerical integration one carries out is actually accurate?

Hence the goal of this part of the research is twofold. First, we need to seek a test problem that has a source term that is highly peaked at the origin and that has an analytic, closed form solution, and we need to study both the SUPG method and the integration approach against the test problem as to the pros and cons and limitations of the two methods. Second, working within the limitations of these methods, we need to obtain the temperature field solutions for the problem of dynamic crack growth and carefully compare the solutions with each other, so as to assure ourselves that the temperature fields we obtained are mathematically accurate and reliable. This section discusses the test problem and make comparisons

between the numerical solutions and the exact analytic solutions.

The test problem must be specified for an infinite domain, so that the integration method can be applied. Note also that T must be zero at infinity. Such a problem is given here for the governing equation (6), with a source term of the form

$$D(x_1, x_2) = 2AB[-2+cx + 2A(x_1^2+x_2^2)]\exp[-A(x_1^2+x_2^2)] \quad (16)$$

where $A(A > 0)$ and B are constant parameters and c is the dimensionless flow velocity in equation (6). To simulate a crack growing in the positive x_1 direction we will consider only negative c values. By adjusting the value of the parameter A, the source term can be made to vary from a very smooth to a strongly peaked function. The exact solution of this problem is given by

$$T(x_1, x_2) = B\exp[-A(x_1^2+x_2^2)]. \quad (17)$$

It is noted again that the analytic solution is independent of the nondimensional flow velocity c, which is convenient for studying the effect of c on the accuracy of the numerical solutions.

The above problem is solved with both the SUPG method and the numerical integration method. In the latter approach the distribution of T is obtained from equation (16) with an adaptive Simpson's scheme. This numerical integration scheme can automatically determine the partitioning of the integration intervals according to the features of the integrand. In places where the integrand is relatively flat, fewer and larger intervals are used, while in places where the integrand has steep slope, more and smaller intervals are used instead. This scheme is extended to two dimensions here, which outperforms other techniques such as the Gauss quadrature.

We have studied the test problem for a variety of parameter values for A, B and c. The results show that the SUPG method with the mesh shown in Fig. 2 consistently yields very accurate solutions for all parameter values, while the accuracy and reliability of the numerical integration approach are very sensitive to the value of the parameter c and to the computer precision or the number of digits used to represent a number on the computer. It is found that, for a fixed computer precision, meaningful solutions cannot be obtained with the numerical integration method when $|c|$ is above a certain value, even though an automatic adaptive scheme is used. As an example, we will look at the case when $A = 50$ and $B = 10^5$ and concentrate on the solution at the point (0.0, 0.1), where the exact solution is $T = 60653$. The results show that, if 64 digits are used to represent a real number on a computer, the integration solution becomes unacceptable when $|c|$ is somewhat larger than 1×10^3. If 128 digits are used, the upper limit for $|c|$ can be pushed up to a value somewhere above 1.25×10^5. In this regard, we note that the problem of dynamic crack growth involves c values just below this upper limit. Accordingly, one might be able to use the numerical integration approach and obtain reasonable solutions, depending on the crack speed and the physical properties of the material in which the crack is propagating. Thus for such cases the integration method can be used as an independent mathematical tool for checking the adequacy of the solution obtained by the SUPG method. It is worth emphasizing that because of its sensitivity to the value of c, the numerical integration approach in general will yield less accurate solution than the SUPG method. Our study also reveals that the SUPG method is much more efficient than the numerical integration approach. Since SUPG only needs to use 32-bit digital precision while the numerical integration usually requires 64 bits for similar accuracy, the SUPG method is found to be at least 10 times faster than the numerical integration approach.

4. CRACK-TIP TEMPERATURE FIELDS

The distribution of temperature increase associated with dynamic crack growth in AISI 4343 steel plate specimens has been computed in this study for five crack propagation speeds, ranging from Mach number $m = 0.1$ to $m = 0.35$, which corresponds to actual crack speeds of $v = 320$ m s^{-1} to $v = 1120$ m s^{-1}. The specimens are heat treated (quenched and tempered) to produce an initial tensile yield strength of $\sigma_0 = 1.49$ GPa. The steel exhibits only a weak strain hardening behavior, which is approximated here with a bilinear stress–strain curve, with the ratio of the plastic line slope vs the elastic line slope being equal to 0.05. Other physical properties of the steel are: $E = 200$ GPa, $c_s = 3200$ m s^{-1}, $k = 38.1$ W m K^{-1}, $\alpha = 1 \times 10^{-5}$ m^2 s^{-1}. For this material, the value of the stress intensity factor K during dynamic crack growth has been found to depend on the crack speed Mach number m in a one-to-one manner [28, 21]. The experiments in [28] show that when $m = 0.22$, $K = 90\,\text{MPa}\sqrt{m}$. In this study, the values of K at other m values are obtained according to the theoretical curve obtained in [21], which is shown in Fig. 5 along with the experimental

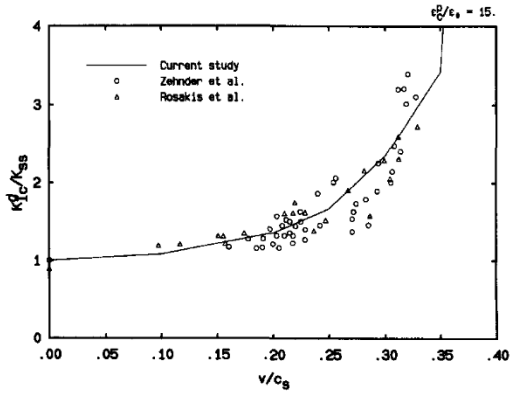

Fig. 5. Relationship between the dynamic stress intensity factor during crack propagation and the crack growth speed, where the solid line is predicted theoretically [21] and the symbols are from experimental measurements [28, 34].

Table 1. A comparison between SUPG and integration method

	SUPG	Integration
T at the crack tip	394.7 K	385.1 K
T_{max}	429.3 K	426.9 K
Location of T_{max}	$(-3.7\times10^{-5}, 0)$	$(-3.7\times10^{-5}, 0)$
T at $(-4.5, 0)$	56.3 K	57.0 K

measurements reported in [28] and [33]. A 90% conversion rate between the plastic work and heat generated is assumed. Other computation aspects have been discussed in earlier sections.

4.1. *Comparison with numerical integration approach*

Both the SUPG and the numerical integration codes are run on a CRAY Y-MP supercomputer at the San Diego Supercomputer Center. The SUPG program uses single precision (64-bits) and each run takes less than 20 s CPU time, while the integration program requires double precision and each run uses more than 600 s. The comparisons shown below are for the case of $m = 0.3$.

Table 1 lists the numerical solutions of the two methods for several items of interest, and Fig. 6 presents the variation of the temperature field along the x_1-axis. We believe that the difference between the two solutions right ahead of the crack tip (see Fig. 6) is caused by error in the numerical integration solution. Although both results show a steep temperature slope at the crack tip, the numerical integration solution failed to predict a temperature rise in the rest of the crack-tip active plastic zone, which extends to about $x = 0.22$ ahead of the crack tip in the nondimensional coordinates. This is probably due to its inability to integrate accurately the integrand right ahead of the crack tip when the variation of the integrand is very steep, which is exactly the case when the point where temperature is being calculated is close to the source points. Except for that minor deviation, the agreement between the two solutions are excellent throughout. Both solutions indicate that the maximum temperature rise is about 428 K and occurs at a point close behind the crack tip, which is consistent with experimental findings in ref. [8].

4.2. *Comparison with experimental measurements*

Shown in Fig. 7 is the variation of the maximum temperature rise (units in degree Kelvin) near the

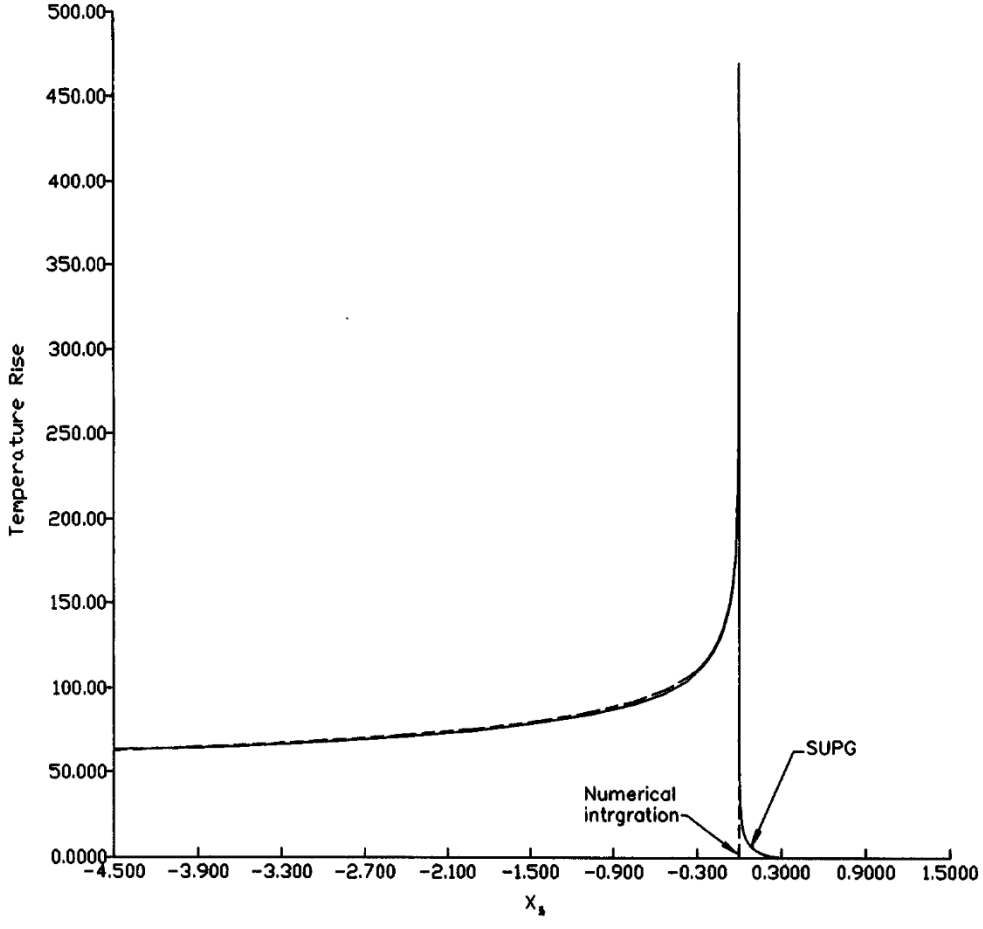

Fig. 6. A comparison of temperature rise along the x_1-axis, between the SUPG formulation and the numerical integration method.

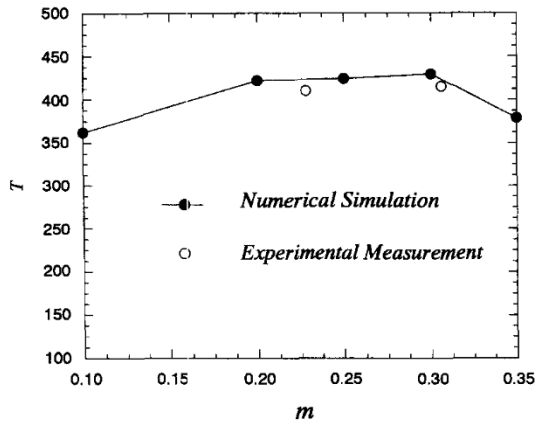

Fig. 7. A comparison of numerically simulated maximum temperature rise for various Mach numbers with experimental measurements from ref. [8].

crack tip with the normalized crack speed m. The numerically simulated results are from the current study and the experimental measurements are from reference [8]. We wish to mention that more than two data points are actually available in ref. [8], but *only the two shown in Fig. 7 are obtained on tempered steel specimens and are from the specimen surface, where plane stress conditions are better approximated than in the machined grooves of the specimens.* It is clear from the comparison that the trend as well as the magnitude of the experimental measurements are well followed by our numerical solutions. However, since the finite element study is 2D by design while the actual deformation and temperature fields are 3D by nature near the crack tip, caution must be exercised in interpreting the above comparison quantitatively until further studies are conducted. For the moment, we should emphasize the qualitative agreement between the two types of data, such as the trend of the temperature variation with the Mach number, and the shape of the temperature contours shown below.

Figure 8 illustrates the temperature contours as predicted by the finite element simulation, and Fig. 9 the contours estimated from temperature measurements in [8, 34]. (Similar contours are also reported in [35].) The contours for Beta-C titanium [Fig. 9(b)] are included because the shape of the contours is mainly determined by the distribution of energy dissipation in the crack-tip active plastic zone. Since the mechanics fields used in this studied, as reported in [19–24], are properly nondimensionalized and in principle can be used to calculate energy dissipations for crack propagation in Beta-C titanium, and since the nondimensional mechanics fields, hence the energy dissipation distributions, are similar in both cases, it is believed that a comparison with the temperature contours of a Beta-C titanium specimen is meaningful. It is seen that, qualitatively, the shapes of the contours are in reasonable agreement with one another. However, quantitatively, the scale of the contour plots are very different. This is not surprising; it is expected

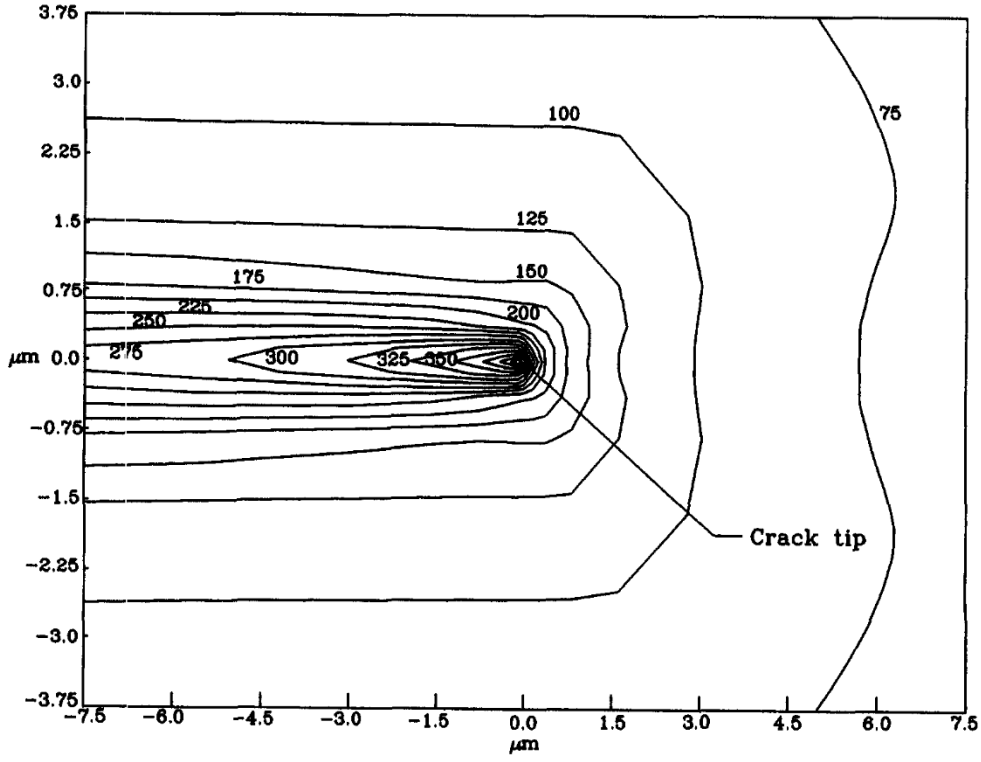

Fig. 8. Temperature contours predicted by the numerical simulation.

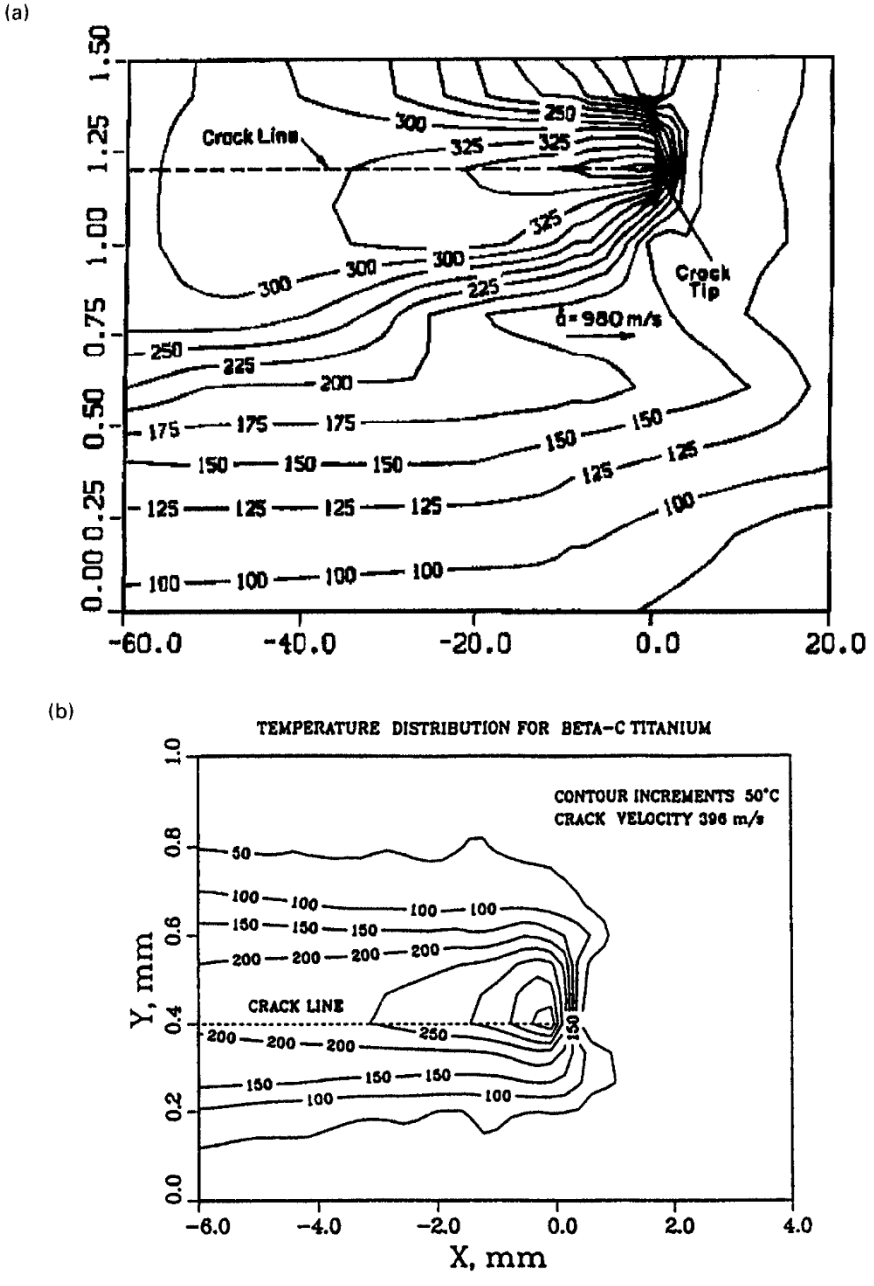

Fig. 9. Experimentally estimated temperature contours from refs [8] in (a) and [35] in (b).

that this 2D, small-strain approximation cannot possibly model all 3D and large deformation phenomena observed experimentally, such as finite plastic deformation near the crack tip and the formation of shear lips near the specimen surfaces. It is believed that the more diffused temperature field observed on the fracture specimen surface reflects the fact that in reality the near-tip materials can relax more effectively than the finite element model, which causes the high crack-tip stresses to spread out, possibly forming a larger plastic zone, and diffusing the dissipated energy into a larger region. What the results of this study demonstrate is that a qualitative modelling of the dynamic fracture process and its temperature field can be achieved with only 2D finite element simulations, and that a quantative comparison can probably be reached with inclusions of large plastic deformation and 3D effects.

5. SUMMARY AND CLOSING COMMENTS

The heat transfer phenomenon induced by crack-tip energy dissipation and local heating during dynamic crack propagation in elastic–plastic solids has been studied with 2D finite element methods and compared with experimental measurements. An uncoupled

approximation has been employed, where a mechanics analysis is performed for the crack-tip stress and deformation fields, from which plastic work rate and heat source distribution are derived, and a thermal analysis is conducted to determine the maximum temperature increase and the spatial variation of the temperature field. The mechanics problem has been solved previously by the authors and the solution is used as input for the current thermal study.

The thermal problem is governed by a convection-dominated flow equation in an Eulerian type description with respect to a moving coordinate system centered at the crack tip. To avoid numerical difficulties related to convection dominated flow equations, the applicability of the Streamline Upwind Petrov–Galerkin formulation to problems with irregularly distributed source terms is investigated carefully. The adequacy of alternative methods, such as the conventional Galerkin formulation and the numerical integration approach, are also studied. These methods are compared with analytical solutions and with one another with regard to their accuracy, reliability, and limitations. Our extensive research results demonstrate that the SUPG formulation consistently gives accurate solutions for all cases studied, while the alternative methods are limited by their ability to yield meaningful solutions, if at all, when the finite element grid Peclet number or the crack growth speed is too large. In particular, it is found that the accuracy of the numerical integration method is very sensitive to the computer precision available, and it costs much more than the SUPG method.

Besides demonstrating the mathematical accuracy and relibility of the numerical codes developed in this study, we have shown that the physical models used in the numerical simulation is able to predict reasonably well what is observed in actual dynamic fracture tests. It is incredible that the maximum temperature rise predicted by the numerical methods matches closely, both in magnitude and in trend, with those obtained from experimental measurements. It is also seen that the shapes of the crack-tip temperature contours resemble those estimated experimentally. It is believed that the differences between the scales of the temperature contours are due to modelling limitations of the current study, which adopted a number of simplifying assumptions. Three-dimensional finite element studies that incorporate finite strain and strain rate and temperature dependent material properties appear to hold high promise for modelling dynamic fracture tests and for predicting thermo-mechanical phenomena associated with dynamic crack propagation in engineering structures.

Finally, it must be pointed out that the effect of finite-speed heat propagation and the possible formation of shock wave around a rapidly propagating crack are not considered in this study. As discussed in a series of papers by Tzou [16–18] using an asymptotic expansion method, thermal shock wave will form when the speed of the moving heat source is equal to or higher than that of the heat propagation. To the authors' knowledge, there is yet no full-field numerical investigation of this thermal shock phenomenon associated with dynamic crack propagation. As noted by Tzou [16–18], the governing equation for this problem will change its characteristics when the heat propagation speed is equal to or higher than the crack growth speed, which may require a different numerical approach. The authors believe that this is an important subject and that more studies, such as full-field finite element investigations, are necessary.

Acknowledgements—The authors wish to thank Dr Alan T. Zehnder for helpful discussions. W. L. and X. D. would also like to thank the University of South Carolina and its College of Engineering for their financial support of this project. The finite element computation was carried out on CRAY Y/MP of the San Diego Supercomputer Center and on the University of South Carolina College of Engineering's mainframe VAX computers.

REFERENCES

1. W. S. Farren and G. I. Taylor, The heat developed during plastic extension of metals, *Proc. R. Soc. Lond. A* **107,** 422–451 (1925).
2. G. I. Taylor and H. Quinney, The latent energy remaining in a metal after cold working, *Proc. R. Soc. Lond. A* **143,** 307–326 (1934).
3. M. B. Bever, D. L. Holt and A. L. Titchener, *The Stored Energy of Cold Work*. Pergamon Press, New York (1973).
4. W. Döll, An experimental study of the heat generated in the plastic region of a running crack in different polymeric materials, *Engng Fracture Mech.* **5,** 259–268 (1973).
5. K. N. G. Fuller, P. G. Fox and J. E. Field, The temperature rise at the tip of fast-moving cracks in glassy polymers, *Proc. R. Soc. Lond. A* **341,** 537–557 (1975).
6. R. Weichert and K. Schönert, Heat generation at the tip of a moving crack, *J. Mech. Phys. Solids* **26,** 151–161 (1978).
7. J. D. Bryant, D. D. Makel and H. G. F. Wilsdorf, Observations on the effect of temperature rise at fracture in two titanium alloys, *Mater. Sci. Engng* **77,** 85–93 (1986).
8. A. T. Zehnder and A. J. Rosakis, On the temperature distribution at the vicinity of dynamically propagating cracks in 4340 steel, *J. Mech. Phys. Solids* **39,** 385–415 (1991).
9. J. R. Rice and N. Levy, Local heating by plastic deformation at a crack tip. In *Physics of Strength and Plasticity* (Edited by A. S. Argon), pp. 277–293. MIT Press, (1969).
10. A. T. Zehnder, A model for the heating due to plastic work, *Mech. Res. Commun.* **18,** 23–28 (1991).
11. R. Weichert and K. Schönert, On the temperature rise at the tip of a fast running crack, *J. Mech. Phys. Solids* **22,** 127–133 (1974).
12. Z-B. Kuang and S. N. Atluri, Temperature field due to a moving heat source: a moving mesh finite element analysis, *J. Appl. Mech.* **52,** 274–280 (1985).
13. Z. L. Li, J. L. Yang and H. Lee, Temperature fields near a running crack tip, *Engng Fracture Mech.* **30,** 791–799 (1988).
14. A. S. Douglas and H. U. Mair, The temperature field surrounding a dynamically propagating mode III crack, *Scripta Metall.* **21,** 479–484 (1987).
15. J. C. Sung and J. D. Achenbach, Temperature at a propagating crack tip in a viscoplastic materials, *J. Thermal Stress* **10,** 243–262 (1987).

16. D. Y. Tzou, Thermal shock waves induced by a moving crack, *ASME J. Heat Transfer* **112,** 21–27 (1990).
17. D. Y. Tzou, Shock wave formation around a moving heat source in a solid with finite speed of heat propagation, *Int. J. Heat Mass Transfer* **32,** 1979–1987 (1989).
18. D. Y. Tzou, The thermal shock phenomena induced by a rapidly propagating crack tip: experimental evidence, *Int. J. Heat Mass Transfer* **35,** 2347–2356 (1992).
19. X. Deng, Dynamic crack propagation in elastic-plastic solids, Ph.D. Thesis, California Institute of Technology, Pasadena, CA (1990).
20. X. Deng and A. J. Rosakis, Negative plastic flow and its prevention in elastic-plastic finite element computation, *Finite Elements Anal. Des.* **7,** 181–191 (1990).
21. X. Deng and A. J. Rosakis, Dynamic crack propagation in elastic–perfectly plastic solids under plane stress conditions, *J. Mech. Phys. Solids* **39,** 683–722 (1991).
22. X. Deng and A. J. Rosakis, A finite element investigation of quasi-static and dynamic asymptotic crack tip fields in hardening elastic–plastic solids under plane stress—I. Crack growth in linear hardening materials, *Int. J. Fracture* **57,** 291–308 (1992).
23. X. Deng and A. J. Rosakis, A finite element investigation of quasi-static and dynamic asymptotic crack tip fields in hardening elastic–plastic solids under plane stress—II. Crack growth in power-law hardening materials, *Int. J. Fracture* **58,** 137–156 (1992).
24. X. Deng, A. J. Rosakis and S. Krishnaswamy, Dynamic crack propagation in elastic–plastic solids under non-K-dominance conditions, *Eur. J. Mech. A Solids* **13,** 327–250 (1994).
25. T. J. R. Hughes and A. Brooks, A multidimensional upwind scheme with no crosswind diffusion. In *Finite Element Methods for Convection Dominated Flows* (Edited by T. J. R. Hughes), ASME-AMD-Vol. 34 (1979).
26. A. N. Brooks and T. J. R. Hughes, Streamline upwind/Petrov–Galerkin formulations for convection dominated flows with particular emphasis on the incompressible Navier–Stokes equations, *Computer Meth. Appl. Mech. Engng* **32,** 199–259 (1982).
27. J. Donea, Generalized Galerkin methods for convection dominated transport phenomena, *Appl. Mech. Rev.* **44,** 205–214 (1991).
28. A. T. Zehnder and A. J. Rosakis, Dynamic fracture initiation and propagation in 4340 steel under impact loading, *Int. J. Fracture* **43,** 271 (1990).
29. I. Christie, D. F. Griffiths, A. R. Mitchell and O. C. Zienkiewicz, Finite element methods for second order differential equations with significant first derivatives, *Int. J. Numer. Meth. Engng* **10,** 1389–1396 (1976).
30. O. C. Zienkiewicz and R. L. Taylor, *The Finite Element Methods*. McGraw-Hill, London (1989).
31. H. S. Carslaw, *Conduction of Heat in Solids*, pp. 267–270. Clarendon Press, Oxford (1959).
32. M. Abramowitz and I. A. Stegun, *Handbook of Mathematical Functions*, Applied Mathematics Series, No. 55, National Bureau of Standards (1972).
33. A. J. Rosakis, J. Duffy and L. B. Freund, The determination of dynamic fracture toughness of AISI 4340 steel by the shadow spot method, *J. Mech. Phys. Solids* **32,** 443–460 (1984).
34. A. T. Zehnder and J. A. Kallivayalil, Temperature rise due to dynamic crack growth in Beta-C titanium, Research Report, Department of Theoretical and Applied Mechanics, Cornell University, Ithaca, New York (1991).
35. J. A. Kallivayalil and A. T. Zehnder, Measurement of the temperature field induced by dynamic crack growth in beta-C titanium, *Int. J. Fracture* (in press).